Proceedings of the 11th
KACC, October 1996

Experimental Study on Impedance Characteristics of a Human Upper Link in a Positioning Motion

° Hideaki Kobayashi*, Hikaru Inooka*, Ryojun Ikeura**

*Dept. of System Information Sciences, Tohoku University, Aoba-ku, Sendai 980-77, JAPAN
Tel: +81-22-217-7021; Fax: +81-22-217-7019; E-mail: koba@control.is.tohoku.ac.jp

**Dept. of Mechanical Engineering, Mie University, Tsu 514, JAPAN
Tel/Fax: +81-592-31-9668; E-mail: ikeura@ss.mach.mie-u.ac.jp

Abstracts In this paper, we have examined the impedance characteristics of a upper link of human being in a positioning motion. Firstly, we have shown the characteristics of the human arm using a bilinear model. From the bilinear model, we have observed that both the driving torque of the forearm and the visco-elasticity of the elbow joint can be controlled by muscles, respectively. Then, we have defined several indexes to show the impedance characteristics. Using the proposed indexes, we have examined the impedance characteristics in the positioning operation. As a result, we can not observe the difference of the impedance characteristics, even if the ease of the positioning motion is varied.

Keywords Electromyogram, Impedance characteristics, Positioning motion, Musculoskeletal System, Muscle

1. INTRODUCTION

Usually robots are needed instead of human being to work in factories, or dangerous places where human being can not work. Recently, robots are needed to help human being in medical institutions and welfare facilities. In the man-machine interactions like in the medical or welfare applications, the robots are necessary to be safe rather than high performance. Therefore, the controller of such robot is different from the industrial robots. Impedance is often used to describe the mechanical characteristics of the human arm[1][2] and the impedance parameter can be changed[2]. It is expected that human being operate safely by changing the impedance. It is reported that man-machine interaction is modeled using the experimentally estimated human arm impedance to design the control system[3][4]. Therefore, it is expected that the impedance characteristics of human arm is effective to design the controller for the medical and welfare robots. In this paper, we examine the impedance characteristics of a upper link of human being in a positioning motion.

In the first section, we have shown the characteristics of the human arm using a bilinear model. From the bilinear model, we observed the difference of the forces controls the driving torque of the forearm, but the sum of the forces uses to controls the impedance parameters of the elbow joint. In the positioning operation, we have shown the mechanical impedance is small when starting to move the forearm toward the target position but the impedance is large enough to restrain the arm when restraining the forearm at the target position. Then, we have defined several indexes for the impedance characteristics. Using the proposed indexes, we have examined the impedance characteristics in the positioning operation.

2. CHARACTERISTICS OF HUMAN ARM

We have considered one-degree-of-freedom rotation around an elbow as the operation. Figure 1 shows the muscles and bones of a human arm. As only two muscles, biceps brachii and triceps brachii, are used in the rotational operation, the mechanics of the muscles and bones are simple. Therefore, it is easy to analyze the control characteristics of the musculoskeletal system.

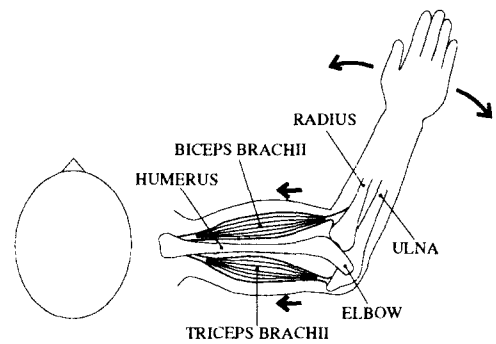

Fig.1 The musculoskeletal system around the elbow

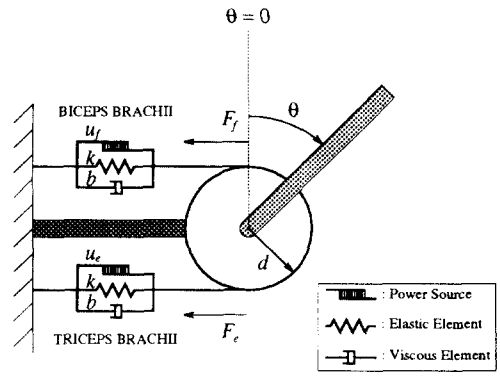

Fig.2 Bilinear model of the musculoskeletal system

Figure 2 shows a model of the musculoskeletal system [7]. From this model, the dynamic equation of the musculoskeletal system is a bilinear model given by

$$I/d \cdot \ddot{\theta} = u_f - u_e - (u_f + u_e)k'\theta - (u_f + u_e)b'\dot{\theta} \quad (1)$$

where I is the inertial momentum of the forearm, d is the length of lever arm, u_f and u_e are the forces of biceps brachii and triceps brachii, respectively, θ is the angle around the elbow, and $k' = kd$ and $b' = bd$, where k and b are constants.

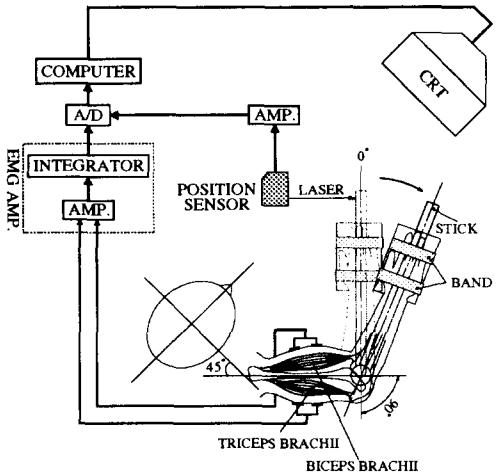

Fig.3 Experimental system

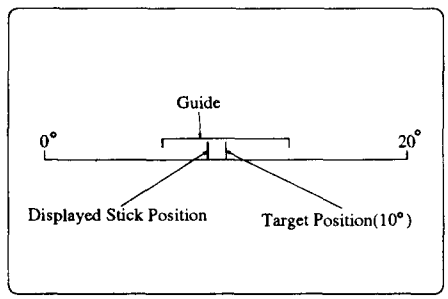

Fig.4 Screen layout

Equation (1) shows that the difference $(u_f - u_e)$ of the forces controls the driving torque of the forearm and the sum $(u_f + u_e)$ of the forces controls the visco-elasticity of the elbow joint, respectively. Since the difference $(u_f - u_e)$ controls the input while the sum $(u_f + u_e)$ controls the system parameters, (1) is nothing but a bilinear system [7].

3. EXPERIMENT

3.1 Experimental devices

The block diagram of the experimental system is shown in Fig. 3. The angle of the stick is measured by a position sensor and the position is displayed on a cathode ray tube (CRT) as shown in Fig. 4. Both the actual stick position and the target position are displayed. The target position was set to 10°. The displacement of the stick is magnified only within the accuracy at the target position. The guide shows the angle of the accuracy. The forces of the biceps brachii and triceps brachii are measured using electromyography. The electromyographic(EMG) signals are passed through an integrator with a time constant of 0.01 s. The sampling intervals of the position and EMG data is 0.01 s.

3.2 Experimental Method

A human operator manipulated a stick as follows (see Fig. 5),

- The human operator started to move the stick position from 0° to the target position (10°), and manipulated the stick so that the position was located in the accuracy at the target position for 2 s. And, the human operator moved to the position at the next start position(20°).
- The human operator started to move the stick position from 20° to the target position (10°), and manipulated the stick so that the position was located in the accuracy at the target position for 2 s. And, the human operator moved to the position at the next start position(0°).

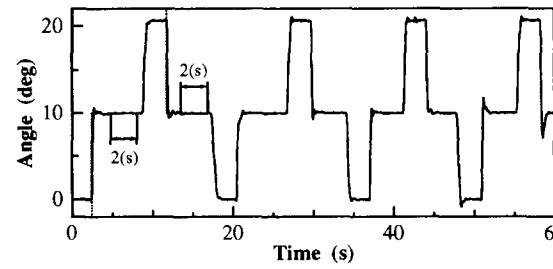

Fig.5 Positioning operation

The time interval of one trial was 60 s.

We set two parameters in the positioning operation , accuracy (A_c) of positioning at the target position and magnification (M_g) of the stick displacement, which are as follows,

- Experiment 1:
  Operation 1(OP_1) : $A_c = \pm 0.5°$, $M_c = 1$
  Operation 2(OP_2) : $A_c = \pm 0.05°$, $M_c = 100$
- Experiment 2:
  Operation 1(OP_1) : $A_c = \pm 0.5°$, $M_c = 1$
  Operation 2(OP_2) : $A_c = \pm 0.5°$, $M_c = 20$

OP_1 is easier than OP_2. OP_1, OP_2 was repeated three times in each experiment, respectively.

3.3 Method for the estimation of muscle force

We have estimated the muscle force by calibrating the measured EMG signals with reference to the bilinear model (1) of the musculoskeletal system. We have assumed that the EMG signals are proportional to the muscle forces as reported in Jacobsen et al. (1982) and Wallace (1989). The muscle force u_f and u_e of biceps brachii and triceps brachii are given by

$$u_f = g_1 \cdot r_f \tag{2}$$

$$u_e = g_2 \cdot r_e \tag{3}$$

where r_f and r_e are EMG signals of each muscle, and g_1 and g_2 are constants.

If a torque τ drives the stick and $\theta = \dot{\theta} = \ddot{\theta} = 0$, then (1) can be rewritten as

$$\tau = u_f - u_e \tag{4}$$

Substituting (2) and (3) into (4), one gets

$$\tau = g_1 \cdot r_f - g_2 \cdot r_e \tag{5}$$

For $\tau = \tau_1 > 0$, $r_f = r_{f1}$ and $r_e = r_{e1}$, (5) becomes

$$\tau_1 = g_1 \cdot r_{f1} - g_2 \cdot r_{e1} \tag{6}$$

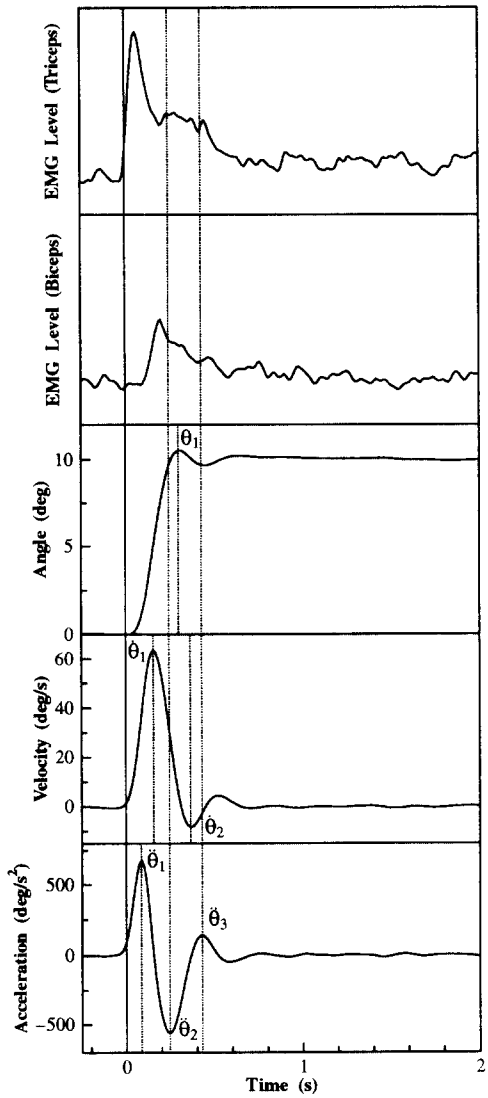

Fig.6 Typical example of movement

Also, for $\tau = \tau_2 < 0$, $r_f = r_{f2}$ and $r_e = r_{e2}$, (5) becomes

$$\tau_2 = g_1 \cdot r_{f2} - g_2 \cdot r_{e2} \tag{7}$$

From (6) and (7), the constants g_1 and g_2 are determined as follows,

$$g_1 = \frac{1}{r_{f1}r_{e2} - r_{e1}r_{f2}}(\tau_1 r_{e2} - \tau_2 r_{e1}) \tag{8}$$

$$g_2 = \frac{1}{r_{f1}r_{e2} - r_{e1}r_{f2}}(\tau_2 r_{f1} - \tau_1 r_{f2}) \tag{9}$$

In this experiment, we have set the torques τ_1 and τ_2 to 1.528 Nm and -1.528 Nm, respectively.

3.4 Method for the estimation of angle

We have estimated the angle θ using the position sensor as follows,

$$\theta = \tan^{-1}\left(\frac{x - x_1}{x_2 - x_1}\tan\theta_t\right) \tag{10}$$

where x is the value of the position sensor when the angle is θ, x_1 and x_2 is the value of the position sensor at 0 ° and 10 °, respectively, and θ_t is 10 °.

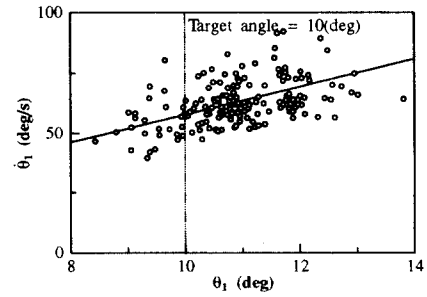

Fig.7 Relation between θ_1 and $\dot{\theta}_1$

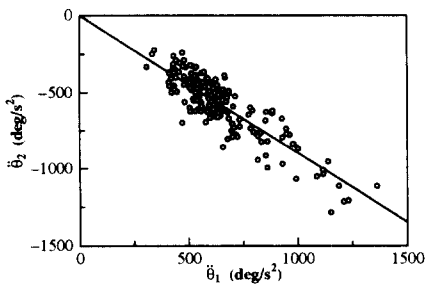

Fig.8 Relation between $\ddot{\theta}_1$ and $\ddot{\theta}_2$

3.5 Experimental Results

We have analyzed the operation when the start position was 0 °. Figure 6 shows a typical example of movement. θ_1 is the first peak angle, $\dot{\theta}_1$ is the maximum velocity and $\dot{\theta}_2$ is the second peak velocity, $\ddot{\theta}_1$ and $\ddot{\theta}_2$ are the maximum and minimum acceleration, respectively, and $\ddot{\theta}_3$ is the third peak acceleration.

As shown in Fig. 6, when starting to move the forearm toward the target position, a large driving torque is generated by the triceps brachii but the activity of biceps brachii is not high. On the other hand, when restraining the forearm at the target position, the activity of both the biceps brachii and the triceps brachii are high. Then, to move the arm easily, it is desirable to make the mechanical impedance as small as possible. Conversely, when bringing the arm to rest, it is desirable to make the impedance large enough to restrain the arm[7].

Firstly, we have shown the characteristics of the positioning operations. In the operation, the overshoot is occurred as shown in Fig. 6. Figure 7 shows the dependence of θ_1 and $\dot{\theta}_1$. We have shown all experimental data. In almost all operation, the overshoot was occurred and θ_1 almost increased in proportion to $\dot{\theta}_1$. Figure 8 shows the relation with $\ddot{\theta}_1$ and $\ddot{\theta}_2$. Figure 8 shows $\ddot{\theta}_1$ is almost proportional to $\ddot{\theta}_2$, and $\ddot{\theta}_2$ is smaller than $\ddot{\theta}_1$. As a result, the human operator move the stick nearby the target very fast but the human operator restrained the stick slowly since the human operator had to place the stick in the accuracy at the target position.

Secondly, we show the characteristics of the accelerating force and restraining force. As shown in Fig. 6, when starting to move the forearm toward the target position, a large driving torque is generated by the triceps brachii, and when restraining the forearm at the target position, the activity of both the biceps brachii and the triceps brachii is

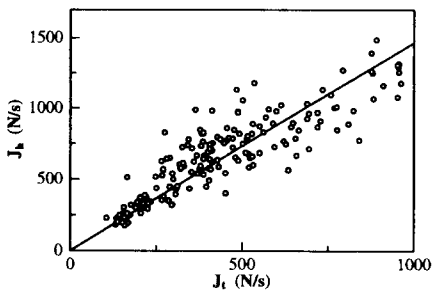

Fig.9 Relation with J_t and J_h

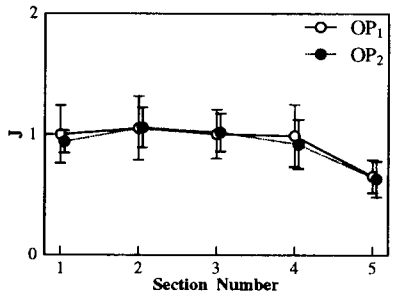

Fig.10 Typical result of J (Experiment 1)

high. We have defined two indexes as follows,

$$J_t = \frac{\int_0^{t(\ddot{\theta}_2)} u_e(t)dt}{t(\ddot{\theta}_2)} \quad (11)$$

$$J_h = \frac{\int_{t(\ddot{\theta}_2)}^{t(\ddot{\theta}_3)} u_f(t) + u_e(t)dt}{t(\ddot{\theta}_3) - t(\ddot{\theta}_2)} \quad (12)$$

where $t(\ddot{\theta}_2)$ and $t(\ddot{\theta}_3)$ is the time at which the acceleration reached $\ddot{\theta}_2$ and $\ddot{\theta}_3$, respectively.

We have shown the results of J_t vs. J_h in Fig. 9. We show all experimental data. Figure 9 shows J_s is almost proportional to J_t. Since,the stiffness of the elbow becomes high when the activity of both the biceps brachii and the triceps brachii is high, it is observed that the high stiffness is needed for the large driving torque. As shown in Fig. 6, the time $[0\ t(\ddot{\theta}_3)]$ is very short. We expected that the movement is carried out under preprogrammed open loop control in this interval[8].

From (1), difference $(u_f - u_e)$ of the forces controls the driving torque of the forearm, but the sum $(u_f + u_e)$ of the forces uses to controls the impedance parameters of the elbow joint. As a result shown in Fig. 9, Then, we have defined following equation for the impedance characteristics.

$$J = \int_{t_1}^{t_2} \frac{u_f(t) + u_e(t) - |u_f(t) - u_e(t)|}{t_2 - t_1} dt \quad (13)$$

We calculate using (13) in follow five section.

- section 1: $[t_1\ t_2] = [0\ \ddot{\theta}_1]$
- section 2: $[t_1\ t_2] = [\ddot{\theta}_1\ \dot{\theta}_1]$
- section 3: $[t_1\ t_2] = [\dot{\theta}_1\ \ddot{\theta}_2]$
- section 4: $[t_1\ t_2] = [\ddot{\theta}_2\ \ddot{\theta}_3]$
- section 5: $[t_1\ t_2] = [\ddot{\theta}_3\ t_e]$

where $t(\dot{\theta}_1)$ is the time at which the velocity reached $\dot{\theta}_1$, $t(\ddot{\theta}_1)$ is the time at which the acceleration reached $\ddot{\theta}_1$, t_e is the time at the end of the operation.

Figure 10 shows the typical result of the experiment 1. All values of the indexes are normalized by dividing by the index value when the section number is 1 in the OP_1. The under or over bars show the standard deviation of the indexes. As shown in the figure, even if the easiness of the positioning was changed,we can not observe the difference of the impedance characteristics. We have same result in the other experiment.

If the human arm is controlled by a simple stiffness control, the higher the accuracy of positioning is, the higher is the stiffness. Therefore, we expect that the human arm is not controlled by such a stiffness control but by a complicated control system of nervous system.

4. CONCLUSIONS

In this paper, we have examined the impedance characteristics of a upper link of human being in a positioning motion. Firstly, we have shown the characteristics of the human arm using a bilinear model. Then, we have defined several indexes to show the impedance characteristics. Using the proposed indexes, we have examined the impedance characteristics in the positioning operation. As a result, we can not observe the difference of the impedance characteristics,even if the ease of the positioning motion is varied. Therefore, we expect that the human arm is not controlled by a simple stiffness control but by a complicated control system of nervous system.

REFERENCES

[1] H. Kazerooni, "Human-Robot Interaction via the Transfer of Power and Information Signals, " *IEEE Trans. on Systems, Man, and Cybernetics*, vol.20, No.2, 450-463, 1990

[2] T. Tsuji, P. Morasso, K. Goto, K. Ito, "Human hand impedance characteristics during maintained posture, " *Biological Cybernetics*, Vol.72, 475-485, 1995

[3] R. Ikeura, M. Monden, H.nooka, "Cooperative motion control of a robot and a human, " *IEEE International Workshop on Robot and Human Communication*, 112-117 (1994)

[4] R. Ikeura, H. Inooka, "Variable Impedance Control of a Robot for Cooperation with a Human, " *IEEE International Conference on Robotics and Automation*, 3097-3102, 1995

[5] G. Wallace, "The Control of Oscillatory Movements of the Forearm, " *Biological Cybernetics*, 61, 233-240, 1989

[6] S. Jacobsen, D. Knutti, R. Johnson, H. Sears, "Development of the Utah Artificial Arm, " *IEEE Trans. on Biomedecal Engineering*, Vol.29, No.4, 249-268, 1982

[7] M. Pecson, K. Ito, Z. Luo, A. Kato, T. Aoyama, M. Ito, "Compliance Control of An Ultrasonic Motor Powered Prosthetic Forearm, " *Proc. of IEEE International Workshop on Robot and Human Communication*, 90-95 1993.

[8] K. Mishima, T. Kurokawa, H. Tamura, "The Bimodal Muscular Control for Very Fast Arm Movements, " *Biomechanics*, VIII-A, 294-300, 1983